

Localized Magnetoplasmon Modes arising from Broken Translational Symmetry in Semiconductor Superlattices

John H. Reina[†], Juan C. Granada[‡] and Neil F. Johnson[†]

[†]*Physics Department, Clarendon Laboratory, Oxford University, Oxford OX1 3PU, U.K.*

[‡]*Departamento de Física, Universidad del Valle, A.A. 25360, Santiago de Cali, Colombia*

(March 10, 2018)

Abstract

The electromagnetic propagator associated with the localized collective magnetoplasmon excitations in a semiconductor superlattice with broken translational symmetry, is calculated analytically within linear response theory. We discuss the properties of these collective excitations in both *radiative* and *non-radiative* regimes of the electromagnetic spectra. We find that low frequency retarded modes arise when the surface density of carriers η_d at the symmetry breaking layer is lower than the density η_0 at the remaining layers. Otherwise ($\eta_d > \eta_0$) a doublet of localized, high-frequency magnetoplasmon-like modes occurs. The corresponding dispersion law and power spectrum of these modes are shown.

I. INTRODUCTION

Much work has been devoted to the study of the properties of low-dimensional heterostructures [1]. Many of the advances are due to the emergence of new crystal growth techniques, such as molecular-beam epitaxy (MBE) and metal organic chemical vapour deposition (MOCVD). These experimental techniques have made possible the fabrication of layered materials with sharp, high-quality interfaces and with dimensions comparable to the electron mean free path and the de Broglie wavelength [2,3]. There are many experimental and theoretical reports concerning the collective excitations that can propagate in such structures, including magnons, plasmons, magnetoplasmons and polaritons [4-17]. Experimental set-ups for detecting some of these collective oscillatory modes have been reported recently [16,17]. Most of the theoretical work in this field is concerned with infinite and semi-infinite superlattices (for a review see [18]). For a periodic array of quantum wells, a plasmon band arises because of the translational symmetry and the long-range electromagnetic coupling of the two-dimensional (2D) electron sheets [8,9,19]. The spectrum of the collective modes becomes richer when an external static magnetic field is applied along the superlattice axis. In particular, low-frequency undamped helicons [10,20–22] and waveguide-like modes [23] can be detected. The case of a semi-infinite semiconductor superlattice was considered by Giuliani and Quinn [11,12,24]. They found a polariton-type plasmon mode (Giuliani-Quinn polariton) which exists only for values of the in-plane wave-vector greater than a certain critical value. This critical value is determined by the differences between the dielectric permittivities of the bulk media and the semi-infinite superlattice. The extension of these works to the case of applied magnetic fields was discussed by Kushwaha [25]. Recently much attention has been paid to the description of the local modes related with the removal of translational symmetry, as for a superlattice with a defect layer [13,26] or a superlattice with a quasiperiodic region following Fibonacci [27] or Cantor [28] sequences. The effects of an applied external magnetic field have also been considered using Green's function techniques [14,30].

Studies of magnetoplasmons in layered heterostructures have mainly focussed on the dispersion law of collective excitations, however the power spectrum of such excitations has not been discussed to our knowledge. In the present work we calculate the retarded photon Green's tensor g_{jk} for the magnetoplasmon modes arising in superlattices with broken translational symmetry. We also discuss the dispersion law (by taking into account retardation effects and the non-homogeneous propagation of these modes) and the power spectra of low-frequency collective excitations.

The outline of the paper is as follows: In Section II we describe the system considered here and obtain analytical expressions for the Green's functions associated with the localized collective oscillations. The corresponding discussion, which is centered on the properties of the collective excitations in both non-radiative and radiative regimes of the electromagnetic spectra, is given in Section III. Analytical and numerical treatments are presented for the cases of *non-retarded* (Sec. III A) and *homogeneous* (Sec. III B) modes of localized magnetoplasmon oscillations. The behavior of the *retarded non-homogeneous* localized modes is discussed in Sec. III C. Conclusions are given in Sec. IV.

II. FORMALISM

We consider an infinite one-dimensional array of quantum wells forming a Type-I superlattice with periodicity d . The z -direction is taken to lie along the superlattice axis. We assume that all the quantum wells are uniformly doped with a surface density of carriers η_0 , except the one centered at $z = 0$ which is doped with a surface density η_d . An external static magnetic field B_0 is applied along the z -direction. We also assume that the distance d between wells is so large that we can neglect wave-function overlap between wells. Therefore the quantum wells are coupled only by the electromagnetic interaction associated with the dynamics of the electron system.

The dynamic magnetoconductivity tensor corresponding to the n 'th layer is given by

$$\sigma_{ij}(n) = \sigma_{ij}^s + (\sigma_{ij}^d - \sigma_{ij}^s)\delta_{n0}, \quad (1)$$

where σ_{ij}^s (σ_{ij}^d) are the components of the 2D dynamic magnetoconductivity tensor associated with the electronic planes with surface density η_0 (η_d). The photon Green's tensor D_{jk} corresponding to the dynamics of the electron system satisfies the following set of differential equations:

$$\begin{aligned} & \left(\frac{\omega^2}{c^2} \epsilon \delta_{ij} - \frac{\partial^2}{\partial x_i \partial x_j} + \nabla^2 \delta_{ij} \right) D_{jk}(\omega; \mathbf{r}_\parallel, \mathbf{r}'_\parallel, z, z') = 4\pi\hbar \delta_{ik} \delta(\mathbf{r} - \mathbf{r}') - \\ & - \frac{4\pi i \omega}{c^2} \Delta(\eta_d) \sigma_{ij} D_{jk}^{(0)}(\omega; \mathbf{r}_\parallel, \mathbf{r}'_\parallel, z') \delta(z) - \frac{4\pi i \omega}{c^2} \sum_{n=-\infty}^{\infty} \sigma_{ij} D_{jk}^{(n)}(\omega; \mathbf{r}_\parallel, \mathbf{r}'_\parallel, z') \delta(z - nd), \end{aligned} \quad (2)$$

where ω is the frequency of the allowed collective excitations, \mathbf{r}_\parallel and \mathbf{r}'_\parallel are vectors in the xy -plane, $\mathbf{r} = (\mathbf{r}_\parallel, z)$ and $\Delta(\eta_d) = \frac{\eta_d}{\eta_0} - 1$. The superscript (n) on the tensor D_{jk} denotes the layer under consideration. Given the homogeneity of the system along the electron layers, we introduce the 2D Fourier transformation

$$D_{jk}(\omega; \mathbf{r}, \mathbf{r}') = \frac{1}{(2\pi)^2} \int d^2 k_\parallel d_{jk}(\omega, \mathbf{k}_\parallel, z, z') e^{i\mathbf{k}_\parallel \cdot (\mathbf{r}_\parallel - \mathbf{r}'_\parallel)}, \quad (3)$$

where \mathbf{k}_\parallel is the in-plane wave vector with components (k_x, k_y) . The isotropy in the xy -plane allows us to perform a coordinate rotation which aligns the x axis with the direction of \mathbf{k}_\parallel . This is achieved by the action of the matrix

$$\hat{S} \equiv \hat{S}(\mathbf{k}_\parallel) = \frac{1}{k_\parallel} \begin{pmatrix} k_x & k_y & 0 \\ -k_y & k_x & 0 \\ 0 & 0 & k_\parallel \end{pmatrix}. \quad (4)$$

Equation (2) hence takes the form

$$\begin{pmatrix} \frac{\omega^2}{c^2} \epsilon + \frac{d^2}{dz^2} & 0 & -ik_\parallel \frac{d}{dz} \\ 0 & \frac{d^2}{dz^2} - \kappa^2 & 0 \\ -ik_\parallel \frac{d}{dz} & 0 & -\kappa^2 \end{pmatrix} \begin{pmatrix} g_{xx} & g_{xy} & g_{xz} \\ g_{yx} & g_{yy} & g_{yz} \\ g_{zx} & g_{zy} & g_{zz} \end{pmatrix} = 4\pi\hbar \delta(z - z') \begin{pmatrix} 1 & 0 & 0 \\ 0 & 1 & 0 \\ 0 & 0 & 1 \end{pmatrix} -$$

$$\begin{aligned}
& \frac{4\pi i\omega}{c^2} \Delta(\eta_d) \begin{pmatrix} \sigma_{xx} & \sigma_{xy} & 0 \\ \sigma_{yx} & \sigma_{yy} & 0 \\ 0 & 0 & 0 \end{pmatrix} \begin{pmatrix} g_{xx}^{(0)} & g_{xy}^{(0)} & g_{xz}^{(0)} \\ g_{yx}^{(0)} & g_{yy}^{(0)} & g_{yz}^{(0)} \\ g_{zx}^{(0)} & g_{zy}^{(0)} & g_{zz}^{(0)} \end{pmatrix} \delta(z) - \\
& \frac{4\pi i\omega}{c^2} \sum_{n=-\infty}^{\infty} \begin{pmatrix} \sigma_{xx} & \sigma_{xy} & 0 \\ \sigma_{yx} & \sigma_{yy} & 0 \\ 0 & 0 & 0 \end{pmatrix} \begin{pmatrix} g_{xx}^{(n)} & g_{xy}^{(n)} & g_{xz}^{(n)} \\ g_{yx}^{(n)} & g_{yy}^{(n)} & g_{yz}^{(n)} \\ g_{zx}^{(n)} & g_{zy}^{(n)} & g_{zz}^{(n)} \end{pmatrix} \delta(z - nd)
\end{aligned} \tag{5}$$

where $g_{jk} = \hat{S}_{jm} d_{mn} \hat{S}_{nk}^{-1}$. In this matrix relation, we introduce the notation $g_{jk} \equiv g_{jk}(\omega, \mathbf{k}_{\parallel}; z, z')$, $g_{jk}^{(n)} \equiv g_{jk(n)} = g_{jk}(\omega, \mathbf{k}_{\parallel}; z = nd, z')$ and $\kappa^2 = k_{\parallel}^2 - \frac{\omega^2}{c^2} \epsilon$.

Without loss of generality, we consider the solutions of Eq. (5) in the region $jd < z < (j+1)d$, with $j \neq 0$ and $0 < z' < d$. The solutions can be represented as follows:

$$g_{ik}(z) = \begin{cases} g_{ik(n)}^+ e^{-\kappa z} + g_{ik(n)}^- e^{\kappa z}, & \text{if } z > 0, \\ \tilde{g}_{ik(n)}^+ e^{\kappa z} + \tilde{g}_{ik(n)}^- e^{-\kappa z}, & \text{if } z < 0, \end{cases} \tag{6}$$

satisfying the following boundary conditions at the n 'th layer:

$$g_{ik(n)}^+ e^{-\kappa d} + g_{ik(n)}^- e^{\kappa d} = g_{ik(n+1)}^+ + g_{ik(n+1)}^-, \tag{7}$$

$$-(1 + \gamma_{xx}) g_{xk(n+1)}^+ + (1 - \gamma_{xx}) g_{xk(n+1)}^- + g_{xk(n)}^+ e^{-\kappa d} - g_{xk(n)}^- e^{\kappa d} = \gamma_{xy} (g_{yk(n+1)}^+ + g_{yk(n+1)}^-), \tag{8}$$

$$-(1 + \gamma_{yy}) g_{yk(n+1)}^+ + (1 - \gamma_{yy}) g_{yk(n+1)}^- + g_{yk(n)}^+ e^{-\kappa d} - g_{yk(n)}^- e^{\kappa d} = \frac{4\pi i\omega}{\kappa c^2} \sigma_{xy} (g_{xk;n+1}^+ + g_{xk;n+1}^-), \tag{9}$$

with

$$\gamma_{xx} = \frac{4\pi i\kappa}{\epsilon\omega} \sigma_{xx}, \quad \gamma_{xy} = \frac{4\pi i\kappa}{\epsilon\omega} \sigma_{xy}, \quad \gamma_{yx} = \frac{4\pi i\omega}{\kappa c^2} \sigma_{yx}, \quad \gamma_{yy} = -\frac{4\pi i\omega}{\kappa c^2} \sigma_{yy}. \tag{10}$$

To solve for the local modes in the superlattice considered here, we assume a solution

$$g_{ik(n)}^{\pm} = g_{ik(0)}^{\pm} \exp(-\alpha|n|d), \tag{11}$$

which decays exponentially as $n \rightarrow \pm\infty$, i.e. far from the electron layer with density η_d ($z = 0$). Equation (11) shows that the attenuation of the fields along the superlattices axis is characterized by the parameter α . The condition for the existence of non-trivial solutions of Eq. (5) in the regions considered above, yields

$$\left(\frac{1}{2} \gamma_{xx} S(\kappa, \alpha) + 1 \right) \left(\frac{1}{2} \gamma_{yy} S(\kappa, \alpha) + 1 \right) = -\frac{\gamma_{xy} \gamma_{yx}}{4} S^2(\kappa, \alpha), \tag{12}$$

where

$$S(\kappa, \alpha) = \frac{\sinh(\kappa d)}{\cosh(\kappa d) - \cosh(\alpha d)} \tag{13}$$

is the superlattice structure factor. Equation (12) is expressed in a general form in terms of the magnetoconductivity tensor σ_{ij} . We employ the local approximation for σ_{ij} :

$$\sigma_{xx} = \sigma_{yy} = i \frac{e^2 \eta_0 \omega}{m(\omega^2 - \omega_c^2)}, \quad \sigma_{xy} = -\sigma_{yx} = \frac{e^2 \eta_0 \omega_c}{m(\omega^2 - \omega_c^2)}. \quad (14)$$

Here $\omega_c = \frac{eB_0}{mc}$ is the cyclotron frequency of the two-dimensional carriers. In this approximation, Eq. (12) takes the form

$$\left(\frac{\kappa d}{2} S(\kappa, \alpha) - \frac{\omega^2 - \omega_c^2}{\omega_p^2} \right) \left(\frac{\omega^2 d \epsilon}{2c^2 \kappa} S(\kappa, \alpha) + \frac{\omega^2 - \omega_c^2}{\omega_p^2} \right) = \left(\frac{\omega_c d \sqrt{\epsilon}}{2c} S(\kappa, \alpha) \right)^2, \quad (15)$$

where $\omega_p = \sqrt{\frac{4\pi e^2 \eta_0}{m \epsilon d}}$ is the three-dimensional plasmon frequency. Equation (15) would be equivalent to that obtained in Refs. [9,10] if $i\alpha$ were to be replaced by a quasi wavenumber. When each quantum well is doped with the same surface density, a magnetoplasma band arises which is related to the periodicity of the system along the superlattice direction. However if $\eta_d \neq \eta_0$ (i.e. if α is a complex number), then $|\cosh(\alpha d)| > 1$: localized magnetoplasmon modes associated with the broken translational symmetry appear on the outside of the bulk magnetoplasmon band.

Following a similar procedure to that described in Ref. [29], it is straightforward to show that the diagonal components of the Green's tensor in the region $-d < z < d$, with $0 < z' < d$, have the following form:

$$g_{xx}(k_{\parallel}, \omega; z, z') = \frac{\pi c^2 \hbar \kappa}{\epsilon \omega^2} f_{xy}(k_{\parallel}, \omega; z, z'), \quad (16)$$

$$g_{yy}(k_{\parallel}, \omega; z, z') = -\frac{\pi \hbar}{\kappa} f_{yx}(k_{\parallel}, \omega; z, z'), \quad (17)$$

$$g_{zz}(k_{\parallel}, \omega; z, z') = -\frac{i k_{\parallel}}{\kappa^2} \frac{d}{dz} g_{xz}(k_{\parallel}, \omega; z, z') - \frac{4\pi \hbar}{\kappa^2} \delta(z - z'), \quad (18)$$

$$g_{xz}(k_{\parallel}, \omega; z, z') = \frac{i\pi \hbar c^2 k_{\parallel}}{\epsilon \omega^2} \zeta_{xz}. \quad (19)$$

In these expressions we have introduced the shorthand notation:

$$f_{ij} \equiv A(\kappa, \alpha) \left\{ B(\kappa, \alpha, z, z') - C(\kappa, \alpha, z) D(\kappa, \alpha, z') \frac{\left[\left(\alpha'_{ii} + \frac{E(\kappa, \alpha, z')}{D(\kappa, \alpha, z')} \right) \alpha_{jj} + F(\kappa, \eta) \right]}{\alpha_{ii} \alpha_{jj} + \frac{1}{2} F(\kappa, \eta)} \right\}, \quad (20)$$

$$\zeta_{xz} \equiv A(\kappa, \alpha) \left\{ G(\kappa, \alpha, z, z') - C(\kappa, \alpha, z) H(\kappa, \alpha, z') \frac{\left[\left(\alpha'_{xx} + \frac{J(\kappa, \alpha, z')}{H(\kappa, \alpha, z')} \right) \tilde{\alpha}_{yy} + F(\kappa, \eta) \right]}{\alpha_{xx} \alpha_{yy} + \frac{1}{2} F(\kappa, \eta)} \right\}, \quad (21)$$

where

$$A(\kappa, \alpha) = \frac{1}{e^{\kappa d} - e^{-\alpha d}}, \quad (22)$$

$$F(\kappa, \eta) = \frac{\gamma_{xy}\gamma_{yx}}{2} [\eta \sinh(\kappa d)]^2, \quad (23)$$

$$\alpha'_{ii}(\kappa, \alpha) = \cosh(\kappa d) - \chi + \eta\gamma_{ii} \sinh(\kappa d), \quad (24)$$

$$\alpha_{ii}(\kappa, \alpha) = \cosh(\kappa d) - \chi + \frac{1}{2}\eta\gamma_{ii} \sinh(\kappa d), \quad (25)$$

$$\tilde{\alpha}_{yy}(\kappa, \alpha) = \cosh(\kappa d) - \chi - \frac{1}{2}\eta\gamma_{yy} \sinh(\kappa d), \quad (26)$$

$$C(\kappa, \alpha, z) = e^{-\alpha d} \sinh(\kappa z) - \sinh[\kappa(z-d)], \quad (27)$$

$$J(\kappa, \alpha, z') = 2 \sinh[\kappa(d-z')] - e^{-\kappa z' - \alpha d}, \quad (28)$$

$$E(\kappa, \alpha, z') = 2 \cosh[\kappa(d-z')] - e^{-\kappa z' - \alpha d}, \quad (29)$$

$$D(\kappa, \alpha, z') = \frac{2 \sinh[\kappa(d-z')] - e^{-\kappa z' - \alpha d}}{\sinh(\kappa d)}, \quad (30)$$

$$H(\kappa, \alpha, z') = \frac{2 \cosh[\kappa(d-z')] - e^{-\kappa z' - \alpha d}}{\sinh(\kappa d)}, \quad (31)$$

$$B(\kappa, \alpha, z, z') = 2 \left[(e^{\kappa d} - e^{-\alpha d}) e^{-\kappa|z-z'|} - e^{\kappa z} e^{-\kappa|d-z'|} \right], \quad (32)$$

$$G(\kappa, \alpha, z, z') = 2 \left[(e^{\kappa d} - e^{-\alpha d}) e^{-\kappa|z-z'|} \text{sgn}(z-z') - e^{\kappa z} e^{-\kappa|d-z'|} \right]. \quad (33)$$

Here $\eta \equiv \frac{\eta d}{\eta_0}$ and $\chi = e^{-\alpha d}$. Notice that the poles of Eqs. (16-18) together with Eq. (15) give the allowed frequencies of the modes which are localized at the defect layer. They can be found analytically in the *non-retarded* limit and for *homogeneous oscillations* in the retarded region. These cases, together with retarded non-homogeneous oscillations, are discussed in the next section.

III. RESULTS AND DISCUSSION

A. Non-Retarded Localized Modes

In the non-retarded region of the spectrum $\omega \ll \frac{ck_{\parallel}}{\sqrt{\epsilon}}$ and the components of the Green's tensor have poles at:

$$\omega^2 = \omega_c^2 + \frac{k_{\parallel} d}{2} \omega_p^2 \left[\coth(k_{\parallel} d) + \Delta(\eta) \left\{ \coth^2(k_{\parallel} d) + \eta(\eta - 2) \right\}^{\frac{1}{2}} \right], \quad (34)$$

$$e^{\alpha d} = \left(1 - \frac{1}{\eta} \right) \cosh(k_{\parallel} d) + \Delta(\eta) \left\{ \left(\frac{1}{\eta} - 1 \right)^2 \cosh^2(k_{\parallel} d) + \left(\frac{2}{\eta} - 1 \right) \right\}^{\frac{1}{2}}. \quad (35)$$

Here $\Delta(\eta) \equiv \Theta(\eta - 1) - \Theta(1 - \eta)$, where $\Theta(x)$ is the Heaviside step function. In order to have a solution describing the local magnetoplasma mode, we need $X \equiv \cosh(\alpha d) > 1$ or $X < 1$. In the non-retarded limit, expression (35) does not depend on the external magnetic field and a solution of X exists for all values of the in-plane wave-vector k_{\parallel} . This behavior contrasts with that of the Giuliani-Quinn surface polariton [11] which can not be excited in the long wavelength region of the spectrum. The above general features are illustrated in Figs. 1 and 2, where we have plotted the dispersion curves $\omega = \omega(k_{\parallel})$ of the localized magnetoplasma

mode for different values of η . The regions between the dashed lines correspond to the allowed frequencies of the magnetoplasmons in the ideal system. It can be seen that the local frequency increases its value with k_{\parallel} . When $k_{\parallel}d \gg 1$, the frequency of the local mode approaches the frequency of the magnetoplasmon oscillations of a single quantum well with surface carrier density ηd . This result is reasonable since the coupling between quantum wells is weak in the $k_{\parallel}d \gg 1$ limit. Figure 1 corresponds to values of $\eta < 1$: in this case $X < -1$ and the local frequencies are lower than those corresponding to the edge of the Brillouin minizone ($X = -1$). The lowest frequency in this case corresponds to ω_c . In the strong coupling limit ($k_{\parallel}d \ll 1$), the local mode has a frequency whose dispersion law can be expressed as

$$\omega = \omega_c + \frac{\pi\sigma_H}{\epsilon d}\eta \left(1 - \frac{\eta}{2}\right) (k_{\parallel}d)^2, \quad (36)$$

where

$$e^{\alpha d} = \frac{1}{2} \left(\frac{1}{\eta} - 1\right) (k_{\parallel}d)^2 - \left(\frac{2}{\eta} + 1\right), \quad (37)$$

with $\sigma_H = \frac{e c \eta_0}{B_0}$. In other words, the behavior of the local low-frequency, non-retarded modes in the strong coupling limit is governed by the Hall conductance of the 2D electron gas σ_H . We might conclude from this analysis that the frequency of this mode is always higher than the cyclotron frequency of the two-dimensional carriers. We will see however that accounting for retardation effects can alter this result drastically.

Figure 2 corresponds to $\eta > 1$. Then $X > 1$ and the local frequencies are higher than those corresponding to the center of the Brillouin minizone ($X = 1$). In the strong coupling limit we have

$$\omega^2 = \omega_c^2 + \omega_p^2 \left[1 + \left(\frac{1}{3} + \frac{\eta}{2}(\eta - 2)\right) (k_{\parallel}d)^2\right], \quad (38)$$

where

$$e^{\alpha d} = 1 + \frac{1}{2} \left(\frac{1}{\eta} - 1\right) (k_{\parallel}d)^2. \quad (39)$$

We see that the frequency of this local mode approaches the three-dimensional value $\sqrt{\omega_p^2 + \omega_c^2}$ as k_{\parallel} approaches zero.

B. Homogeneous Magnetoplasmon Oscillations

In the above discussion we have neglected the role of retardation effects. Now we consider these effects for the $k_{\parallel} = 0$ modes, which corresponds to homogeneous (along the planes) oscillations of the electron system. In this case

$$\omega = \pm\omega_c + \frac{\omega_p^2 d}{2c} \left[\cot \left(\frac{\omega d \sqrt{\epsilon}}{c} \right) + \Delta(\eta) \left\{ \cot^2 \left(\frac{\omega d \sqrt{\epsilon}}{c} \right) - \eta(\eta - 2) \right\}^{\frac{1}{2}} \right], \quad (40)$$

$$e^{\alpha d} = \left(1 - \frac{1}{\eta}\right) \cos \left(\frac{\omega d \sqrt{\epsilon}}{c} \right) + \Delta(\eta) \left\{ \left(1 - \frac{1}{\eta}\right)^2 \cos^2 \left(\frac{\omega d \sqrt{\epsilon}}{c} \right) + \left(\frac{2}{\eta} - 1\right) \right\}^{\frac{1}{2}}. \quad (41)$$

In contrast with previous non-retarded results, the magnitude $e^{\alpha d}$ in the present case shows a dependence on the external magnetic field B_0 . This follows from the fact that the modes

described by Eq. (41) owe their existence to retardation effects. In this sense the origin of these local modes differs markedly from the origin of the non-retarded ones. In the particular case when $|1 - \eta| \ll 1$ we find localized modes with frequencies close to the center or the edge of the Brillouin mini-zone ($X = \pm 1$ respectively). We obtain for these frequencies that

$$\omega = \omega_0 - \Delta(\eta) (1 - \eta)^2 \frac{\omega_p^2 d}{4c\sqrt{\epsilon}} \sin\left(\frac{\omega_0 d \sqrt{\epsilon}}{c}\right), \quad (42)$$

where ω_0 is the frequency at which the local mode enters the bulk band of the waveguide-like magnetoplasmon oscillations which exist in the ideal system [23]. For $\omega_c > \frac{c}{d\sqrt{\epsilon}}$ the frequency ω_0 satisfies the inequality $\omega_0 < \omega_c$. This means, that the local modes have frequencies lower than the electron cyclotron frequency. The above features are illustrated in Figs. 3 and 4, where we have plotted the dependences $\omega = \omega(\eta)$ for different values of the applied external magnetic field.

Figure 3 shows the dependence $\omega = \omega(\eta)$ for the case $\eta_d < \eta_0$. When η_d tends to zero, the local frequency approaches the cyclotron frequency. This means that the absence of carriers at the defect layer leads to the appearance of a local mode with a frequency equal to the cyclotron frequency of the carriers at the remaining layers. We also see that for a fixed value of the surface carrier density η_d at the defect layer, the local frequency increases with the applied magnetic field. For a given value of the external applied magnetic field B_0 , however, ω decreases with increasing η_d . In the case $\eta_d > \eta_0$ the frequencies corresponding to localized modes appear only in the high frequency retarded region (i.e. $\omega \gg \omega_c$). The analysis shows that there exist a large number of doublets of local modes. Figure 4 displays the dependence $\omega = \omega(\eta)$ for the first doublet. For a given value of η_d we found that the frequency of the lowest (highest) component of this doublet decreases (increases) with applied magnetic field. For this reason the separation between the components of the doublet increases considerably with magnetic field.

C. General Dispersion Relations and Power Spectra

We now focuss on the description of the localized modes in the retarded region (i.e. $\omega > \frac{ck_{\parallel}}{\sqrt{\epsilon}}$). Figure 5(a) shows the behavior of the frequency ω (in units of ω_p) as a function of in-plane wave number (in units of $\frac{1}{d}$) for $\eta = 0.5$. The dashed region corresponds to the bulk helicon band. We see that in the forbidden region, a local helicon mode appears which is localized in the vicinity of the bulk band edge. With increasing in-plane wave number k_{\parallel} , the frequency of the local modes rises until it reaches the electron cyclotron frequency; here it loses its local-mode character since its frequency is now indistinguishable from the frequencies describing the layer dynamics in the ideal system. Also we note that if $\eta \rightarrow 1$, the dispersion curves approach the edge of the bulk helicon band; if on the other hand $\eta \rightarrow 0$, it can be seen from the poles of the Green's functions (Sec. II) that the frequency corresponding to the dynamics of the defect layer tends to ω_c for all values of k_{\parallel} . In Fig. 5(b) the first doublet of localized modes corresponding to $\eta = 1.5$ is plotted. The dashed area corresponds to the bulk magnetoplasma band. We see that the lowest mode of the doublet slowly increases its frequency with k_{\parallel} until it reaches the bulk continuum. The other mode of the doublet increases its frequency more rapidly than the lowest mode, and tends to the dispersion relation $\omega = \frac{ck_{\parallel}}{\sqrt{\epsilon}}$ with increasing k_{\parallel} .

The expressions for the diagonal Fourier components of the photon propagator enable us to obtain the peaks corresponding to power spectra of such modes; i.e. the imaginary part of the sum over g_{ii} given by $\text{Im}\sum g_{ii}$ where $i = x, y, z$. In Fig. 6(a) we show the power spectra of the lowest frequency modes for different values of k_{\parallel} , in the regime where the density of carriers at the defect layer satisfies $\eta_d < \eta_0$. Only one peak exists which corresponds to frequencies lower than the cyclotron frequency ω_c . With increasing in-plane wave vector k_{\parallel} , the frequency at the maxima of such peaks shifts to the right until it reaches ω_c . These features are also illustrated in Fig. 5(a). In addition, the frequency corresponding to the peaks in Fig. 6(a) increases when the density of carriers at the defect layer diminishes.

For the case $\eta_d > \eta_0$, there are no peaks with frequencies satisfying $\omega < \omega_c$. In this case the peaks corresponding to localized modes appear in the high frequency retarded region of spectrum. The analysis shows that there exist a large number of doublets of local modes. We limit ourselves to discussion of the features corresponding to the first doublet. In Fig. 6(b) we show the power spectra for different values of k_{\parallel} . In the homogeneous case the separation between the components of the doublet is small in comparison with ω_p and it increases with increasing in-plane wave vector. These results agree with those in Fig. 5(b).

IV. CONCLUSIONS

We have used the formalism of linear response theory in order to consider the localized modes in a Type-I superlattice with broken translational symmetry, in the presence of an external static magnetic field. We found that a low frequency retarded mode arises only when the surface carrier density η_d is lower than the corresponding density η_0 at the remaining layers. This mode has frequencies greater than those corresponding to the edge of the helicon band, but is lower than the cyclotron frequency. In contrast for $\eta_d > \eta_0$, we found a doublet of localized high-frequency magnetoplasmon-type modes. These results can be extended to consider a distribution of defect layers in a Type-I superlattice. In this case it is necessary to take into account the techniques developed for the description of localized states in disordered systems [31]. To our knowledge there are so far no experimental results on superlattices with a single defect layer, however we believe that the localized collective excitations described here can indeed be detected with currently available technology using Raman spectroscopy experiments: similar experiments have been reported recently for the case of GaAs/Al_xGa_{1-x}As double quantum well structures [16], where acoustic and optic plasmon modes of this electron bilayer system were successfully observed using electronic Raman scattering. We hope that the results reported in this paper will stimulate further experimental work on this topic.

J.H.R. thanks the financial support of COLCIENCIAS.

REFERENCES

- [1] Stern F 1993 in *Physics of Low-dimensional Semiconductor Structures*, ed P N Butcher, N H March and M P Tosi (Plenum Press, New York)
- [2] L L Chang L and K Ploog eds 1985 *Molecular Beam Epitaxy and Heterostructure* (Plenum, New York); E H Parker ed 1985 *The Technology and Physics of Molecular Beam Epitaxy Heterostructure* (Plenum, New York)
- [3] Joyce B A 1985 *Rep. Prog. Phys.* **48** 1637
- [4] Bass F G and Bulgakov A A 1997 *Kinetic and Electrodynamical Phenomena in Classical and Quantum Semiconductor Superlattices* (Nova Science Publishers, New York)
- [5] Cottam M G and Tilley D R 1989 *Introduction to Surface and Superlattice Excitations* (Cambridge University Press, Chichester)
- [6] Raj R and Tilley D R 1989 *The Electrodynamics of Superlattices*, in *The Dielectric Function of Condensed Systems* ed R Loudon and D Kirzhnitz (North Holland, Amsterdam)
- [7] Granada J C and Oliveira F A 1990 *Solid State Commun.* **75** 179
- [8] Das Sarma S and Quinn J J 1982 *Phys. Rev. B* **25** 7603
- [9] Bloss W L and Brody E M 1982 *Solid State Commun.* **43** 523
- [10] Tselis A, Gonzalez de la Cruz G and Quinn J J 1983 *Solid State Commun.* **47** 43
- [11] Giuliani G F and Quinn J J 1983 *Phys. Rev. Lett.* **51** 919
- [12] Giuliani G F, Qin G and Quinn J J 1984 *Surf. Sci.* **142** 433
- [13] Bloss W L 1991 *Phys. Rev. B* **44** 1105
- [14] Granada J C 1996 *Braz. J. of Physics* **26** 211
- [15] Wendler L and Grigoryan V G 1999 *J. Phys.: Condens. Matter* **11** 4199
- [16] Kainth D S, Richards D, Bhatti A S, Hughes H P, Simmons M Y, Linfield E H and Ritchie D A 1999 *Phys. Rev. B* **59** 2095
- [17] Moresco F, Rocca M, Hildebrandt T and Henzler M 1999 *Phys. Rev. Lett.* **83** 2238; Grésillon S *et al.* 1999 *ibid.* **82** 4520
- [18] Albuquerque E L and Cottam M G 1993 *Phys. Rep.* **240** 383
- [19] Fetter A L 1973 *Ann. Phys.* **81** 367
- [20] Babiker M 1987 *Solid State Commun.* **64** 983
- [21] Wendler L and Kaganov M I 1986 *Phys. Status Solidi* **K33** 143b
- [22] Vagner I D and Bergman D 1987 *Phys. Rev. B* **35** 9856
- [23] Granada J C, Kosevich A M and Kosevich Yu A 1990 *J. Phys.: Condens. Matter* **2** 6279
- [24] Jain J K and Allen P B 1985 *Phys. Rev. B* **32** 997
- [25] Kushwaha M 1993 *J. Appl. Phys.* **73** 792
- [26] Yibing L and Rocca M 1993 *J. Phys.: Condens. Matter* **5** 6597
- [27] Liu N H, Feng W and Wu X 1992 *J. Phys.: Condens. Matter* **4** 9823
- [28] Liu N H, Feng W and Wu X 1993 *J. Phys.: Condens. Matter* **5** 4623
- [29] Cottam M G and Maradudin A A 1984 *Surface Excitations* ed V M Agranovich and R Loudon (North-Holland, Amsterdam)
- [30] Reina J H and Granada J C 1996 in *Surfaces, Vacuum and their Applications*, Conference Proceedings **378** 137 (American Institute of Physics Press); Reina J H 1994 *Undergraduate Thesis* Universidad del Valle (unpublished)
- [31] Rickayzen G 1988 *Green's Functions and Condensed Matter* (Academic Press, London)

Figure Captions

FIGURE 1. Dispersion curves of the local non-retarded magnetoplasmon modes for different values of the surface carrier density at the defect layer: $\eta \equiv \frac{\eta_d}{\eta_0} = 0.1, 0.5,$ and 0.9 . The regions between the dashed lines correspond to the allowed frequencies of the magnetoplasmons in the ideal system. $\omega_c = 0.014\omega_p$ and $\frac{\omega_p d \sqrt{\epsilon}}{c} = 2.3$.

FIGURE 2. Same as in Fig. 1 but for $\eta = 1.5, \eta = 3.0,$ and 5.0 .

FIGURE 3. Plot of the homogeneous ($k_{\parallel} = 0$) low-lying local magnetoplasmon frequencies as a function of the surface carrier density at the defect layer for $\eta_d < \eta_0$ and for different values of the applied magnetic field: $\omega_c = 0.014\omega_p$ ($B_0 = 1\text{T}$), $0.14\omega_p$ ($B_0 = 10\text{T}$), and $0.41\omega_p$ ($B_0 = 30\text{T}$). $\frac{\omega_p d \sqrt{\epsilon}}{c} = 2.3$.

FIGURE 4. Same as in Fig. 3 but for $\eta_d > \eta_0$.

FIGURE 5. (a) Dispersion curves of the localized magnetoplasma modes (solid lines) for retarded non-homogeneous oscillations ($\omega > \frac{ck_{\parallel}}{\sqrt{\epsilon}}$). $\eta = 0.5$, $\omega_c = 0.014\omega_p$ and $\frac{\omega_p d \sqrt{\epsilon}}{c} = 2.3$. The dashed region corresponds to the bulk helicon band. (b) Same as in Fig. (a) but for $\eta = 1.5$. The dashed area corresponds to the bulk magnetoplasmon band.

FIGURE 6. (a) Power spectra (in arbitrary units) of low-frequency localized magnetoplasmon modes as a function of the excitation frequency and the in-plane wave number in the cases $k_{\parallel}d = 0.0, 0.015$ and 0.025 . Input parameters as in Fig. 5(a). (b) Same as in Fig. (a) but for $k_{\parallel}d = 0.0, 1.0$ and 1.5 . Input parameters as in Fig. 5(b).

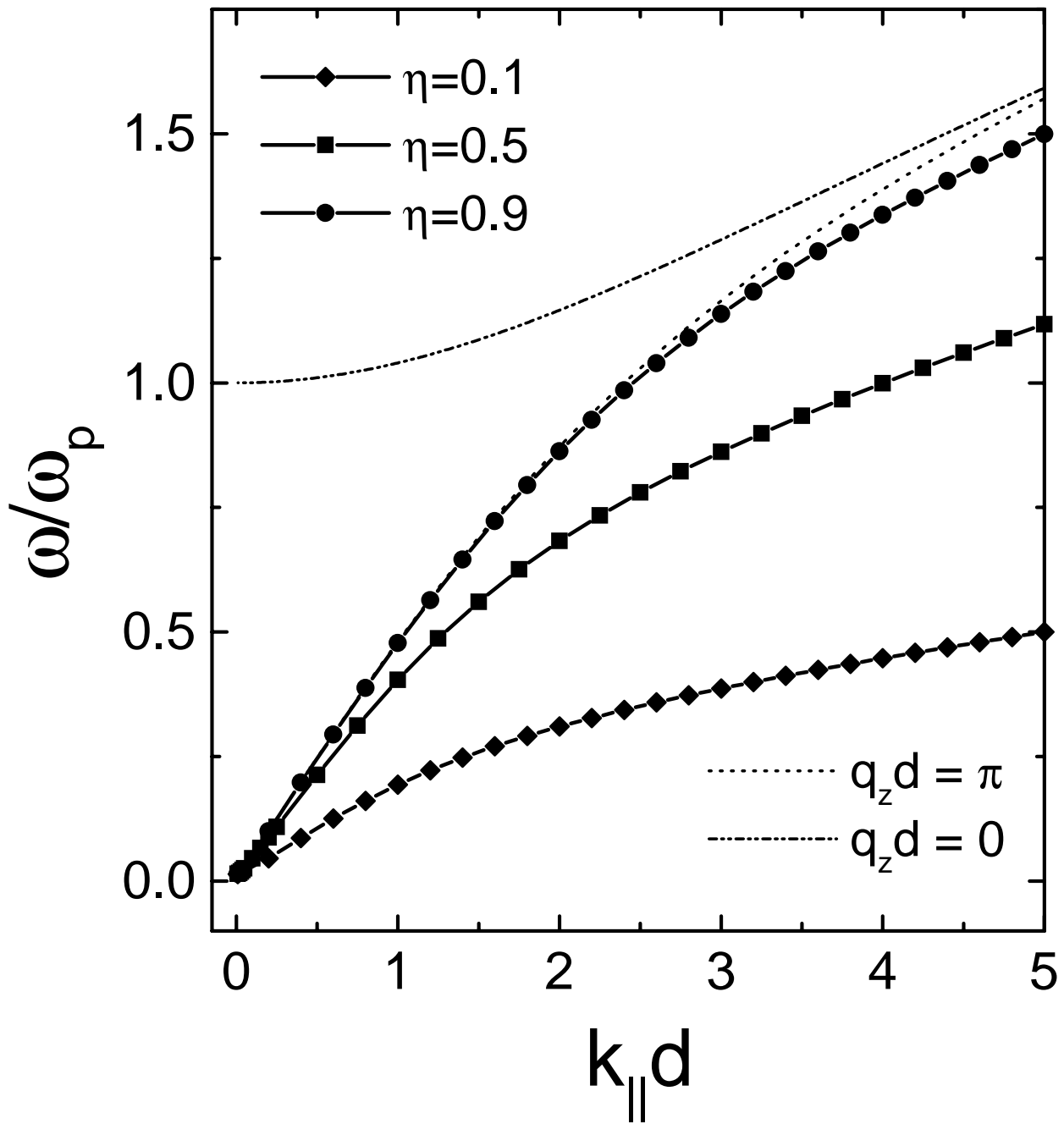


Figure 1

J.H. Reina et al.

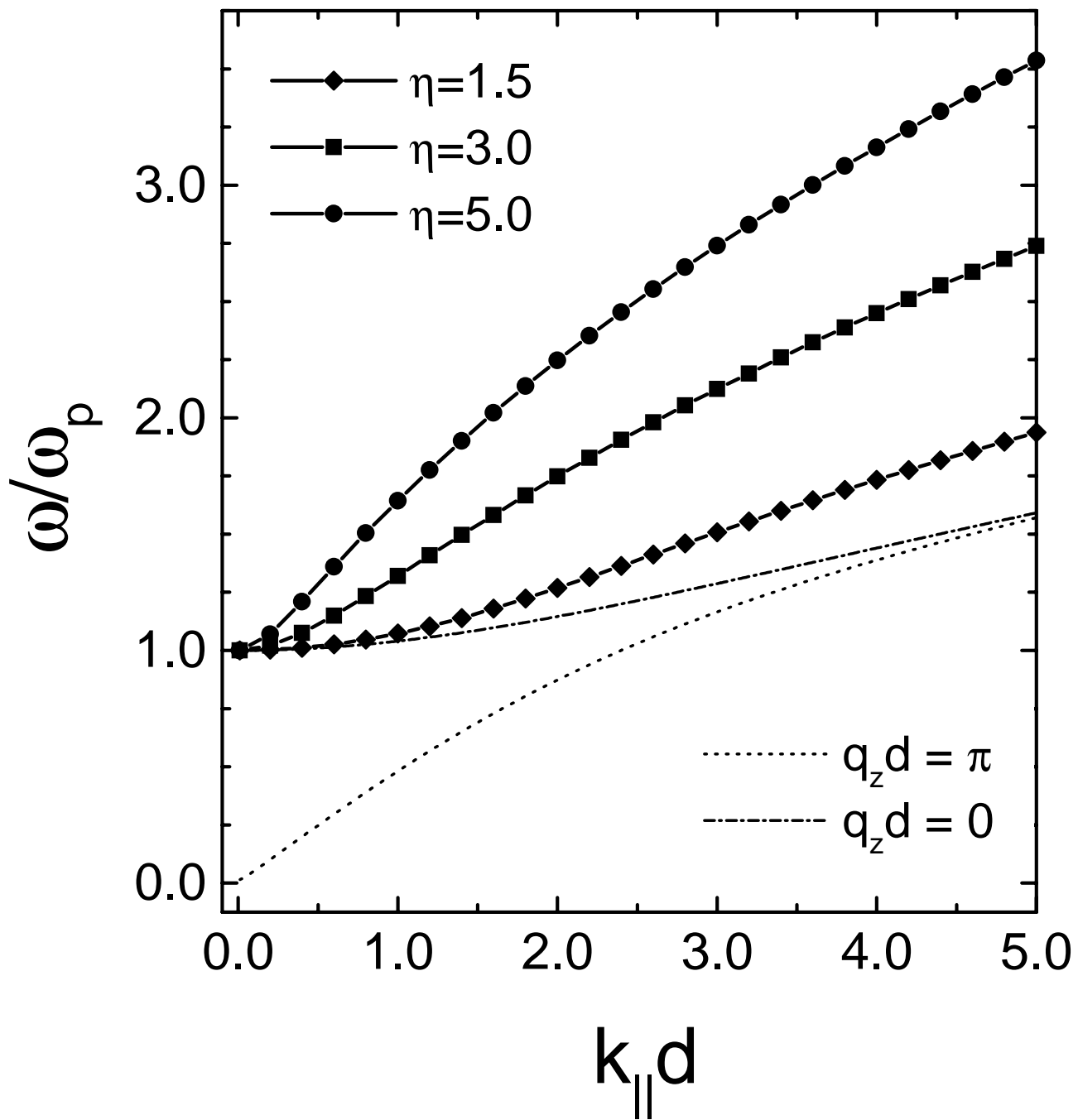


Figure 2

J.H. Reina et al.

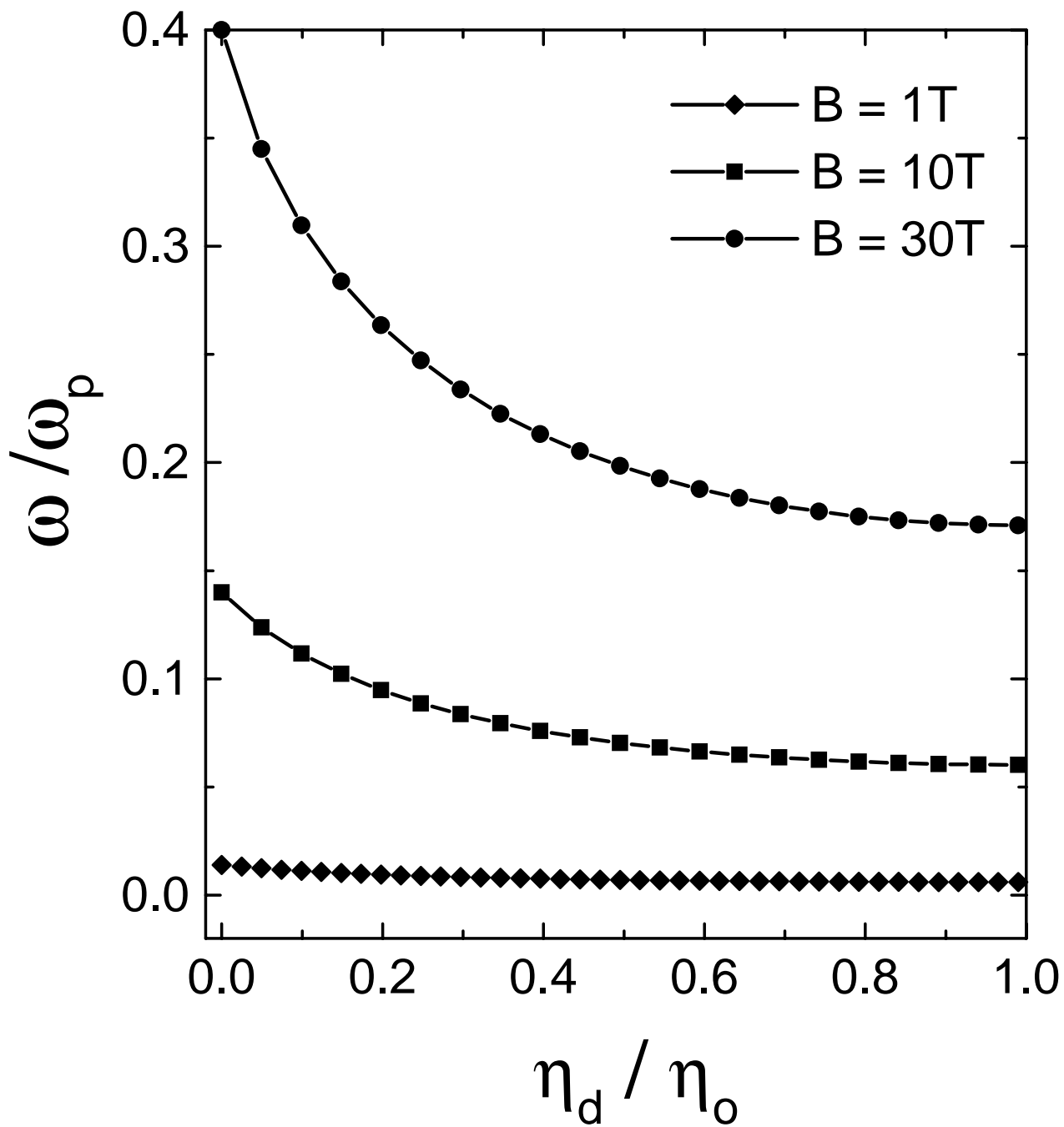


Figure 3

J.H. Reina et al.

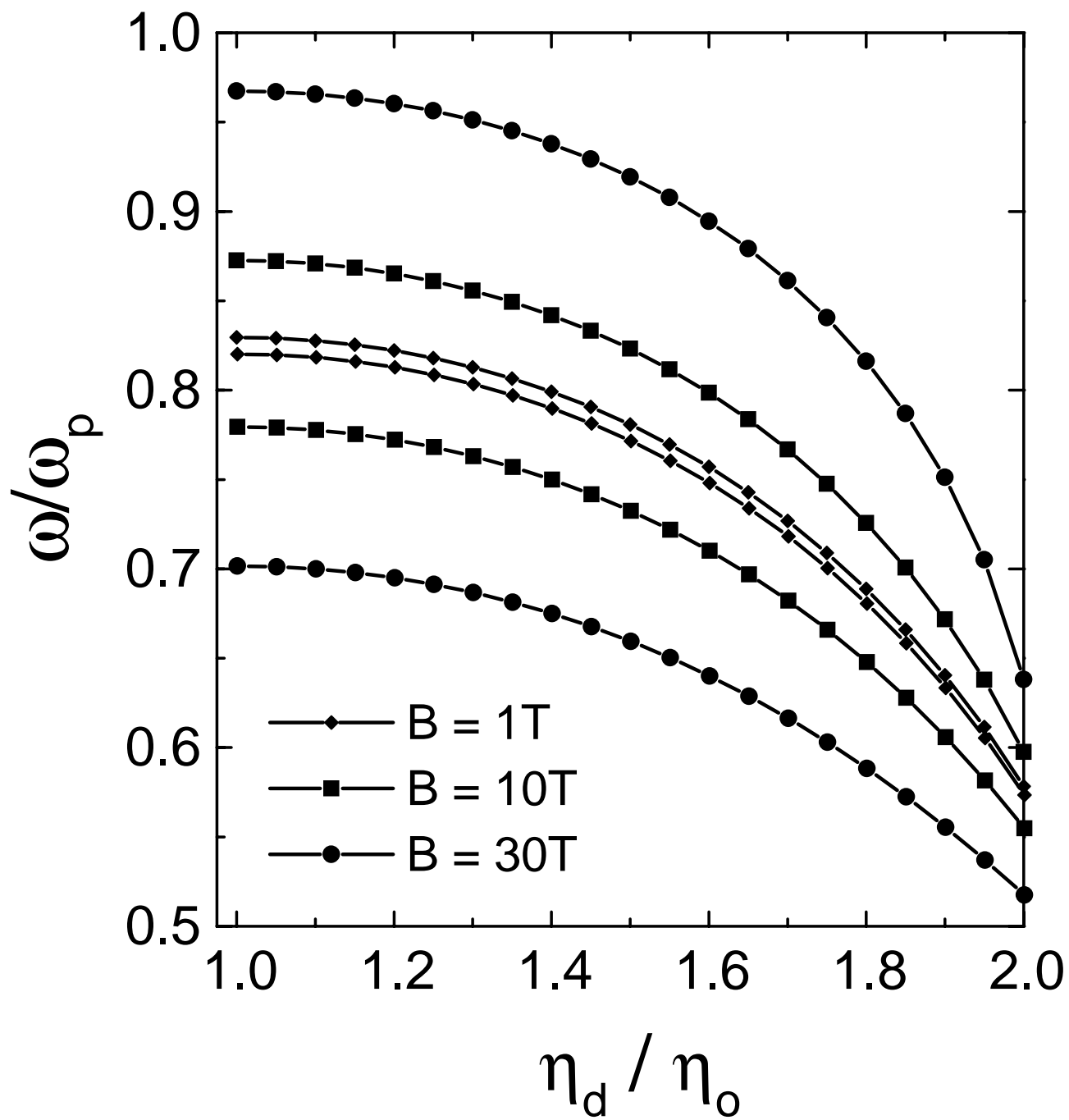


Figure 4
J.H. Reina et al.

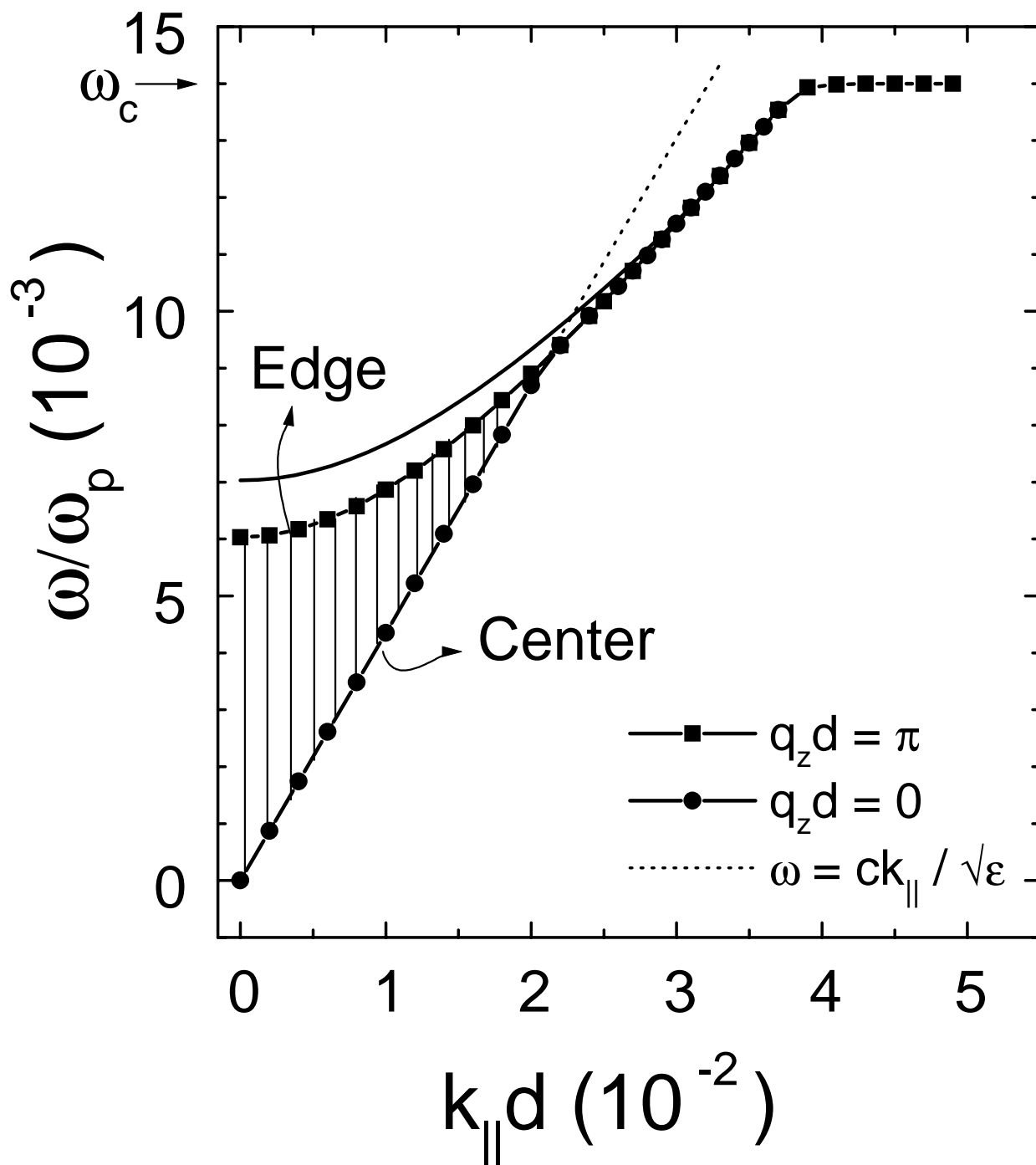


Figure 5(a)
 J.H. Reina et al.

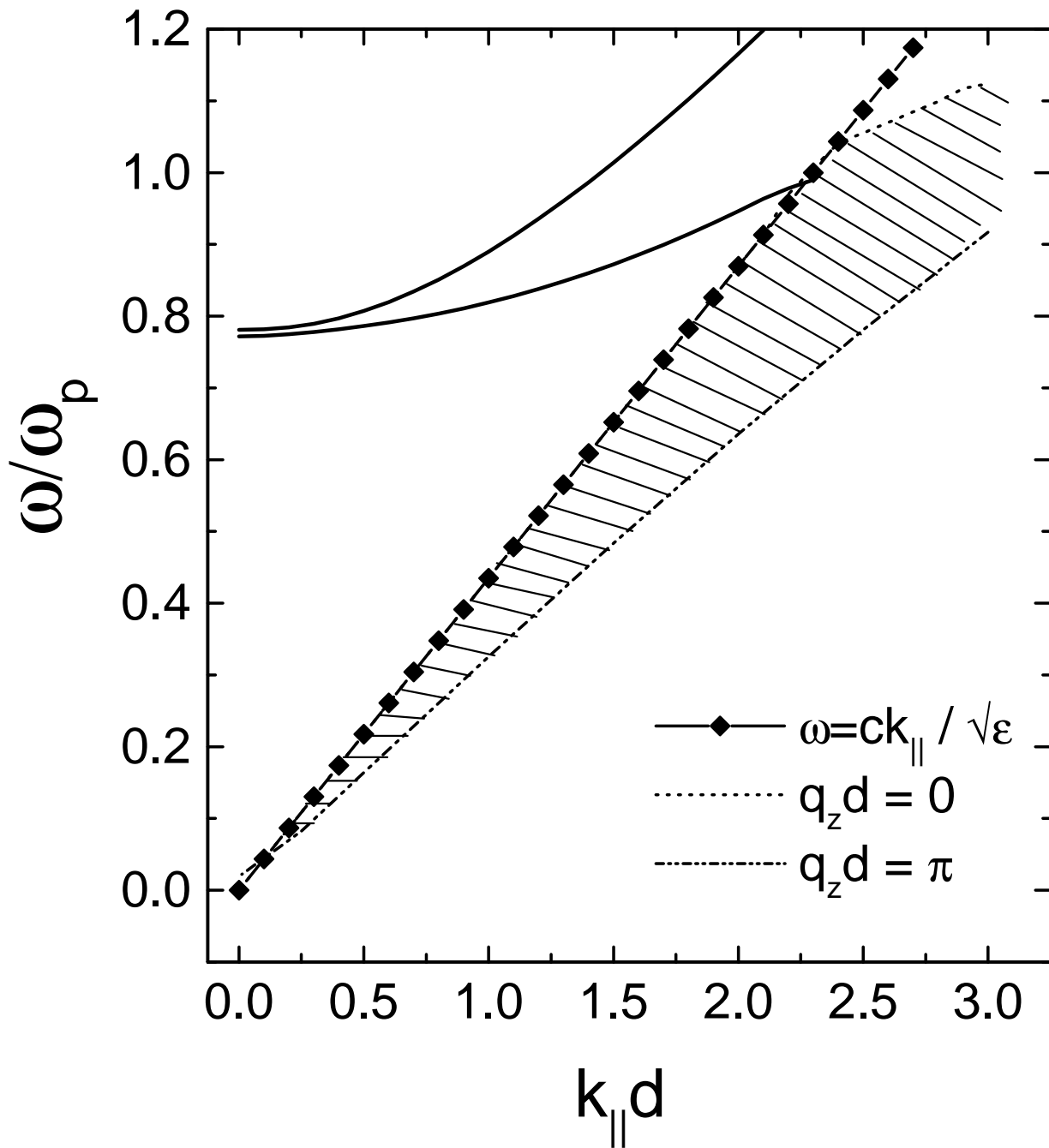


Figure 5(b)
J.H. Reina et al.

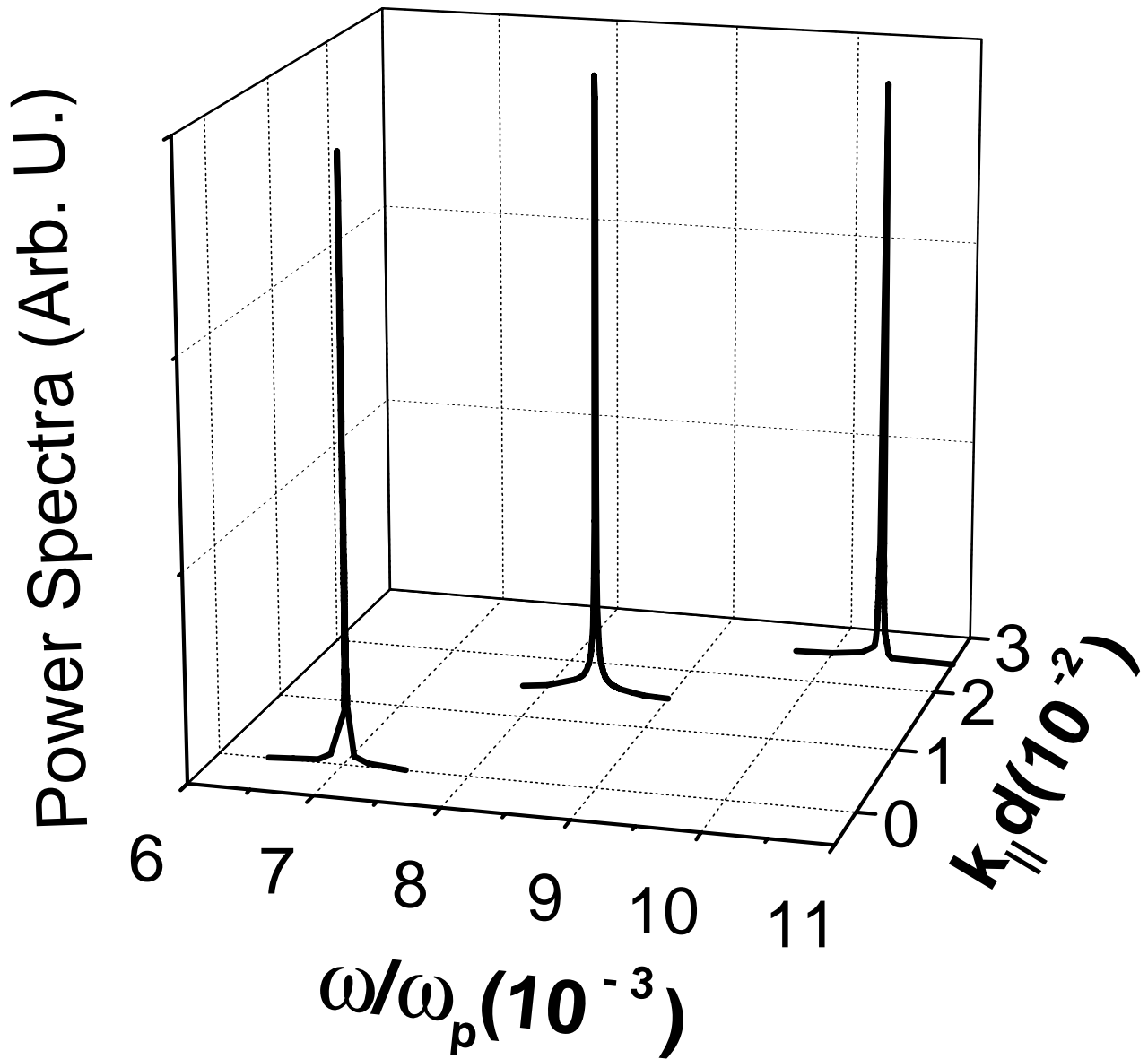


Figure 6(a)

J.H. Reina et al.

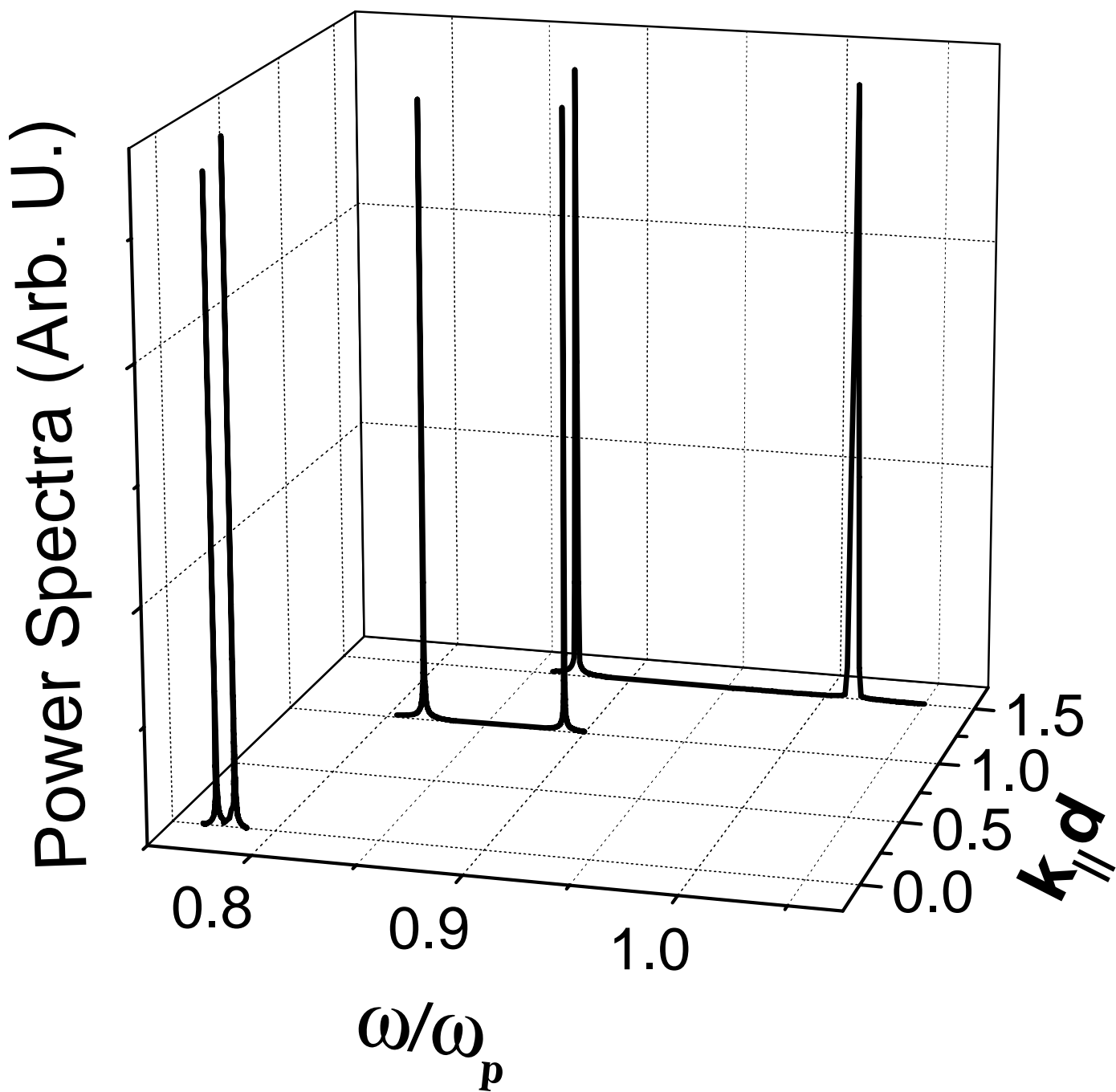


Figure 6(b)
J.H. Reina et al.